PRG 033 ©July 2017

QUEEN'S UNIVERSITY

POLYMERS RESEARCH GROUP

19 Division Street, Kingston, ON, K7L 3N6 Canada

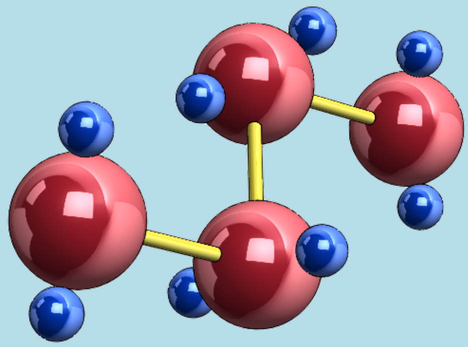

FLUID ELASTICITY IN PLASTIC PIPE EXTRUSION: LOADS ON DIE BARREL

C. Saengow[1,3], A.J. Giacomin[1,2,*]

[1]Chemical Engineering Department
Polymers Research Group
[2]Mechanical and Materials Engineering Department
Queen’s University
Kingston, Ontario, CANADA K7L 3N6

[3]College of Integrated Science and Technology
Rajamangala University of Technology Lanna
Doisaket, Chiangmai, THAILAND 50220

This report is circulated to persons believed to have an active interest in the subject matter; it is intended to furnish rapid communication and to stimulate comment, including corrections of possible errors.

*Corresponding author (giacomin@queensu.ca)

QU-CHEE-PRG-TR--2017-33

LOADS ON DIE BARREL AND FLUID ELASTICITY IN PLASTIC PIPE EXTRUSION

C. Saengow[1,3] and A.J. Giacomin[1,2,*]

[1]Polymers Research Group, Chemical Engineering Department,
[2]Mechanical and Materials Engineering Department
Queen's University, Kingston, ON, CANADA K7L 3N6

[3]College of Integrated Science and Technology
Rajamangala University of Technology Lanna
Doisaket, Chiangmai, THAILAND 50220.

ABSTRACT

In large thick plastic pipe extrusion, the residence in the cooling chamber is long, and the melt inside the pipe sags under its own weight, causing the product to thicken on the bottom (and to thin on the top). To compensate for sag, engineers normally shift the die centerpiece downward. This paper focuses on how this decentering triggers unintended consequences for elastic polymer melts. We employ eccentric cylindrical coordinates, to capture exactly the geometry of our problem, the flow between eccentric cylinders. Specifically, we arrive at an exact analytical expression for the axial and lateral forces on the die barrel using the polymer process partitioning approach, designed for elastic liquids. We choose the Oldroyd 8-constant framework due to its rich diversity of constitutive special cases. Since our main results are in a form of simple algebraic expression along with two sets of curves, they can thus be used not only by engineers, but any practitioner. We close our paper with detailed dimensional worked examples to help practitioners with their pipe die designs.

Keywords: Plastic pipe extrusion; eccentric annular flow; extrusion die design; straw extrusion; catheter extrusion; Oldroyd 8-constant framework.

*Corresponding author (giacomin@queensu.ca)

CONTENTS

TABLES

FIGURES

I. INTRODUCTION

When plastic pipe is solidified, it proceeds through a long cooling chamber (see **Fig. 1.** of [41]). Inside this chamber, inside the hollow extrudate, the plastic is molten, and this inner surface solidifies last. Sag, the flow due to the self-weight of the melt, then transpires in this cooling chamber, and sometimes, thickened regions (called *knuckles*) arise in the lower quadrants, especially of large diameter thick-walled pipes. To compensate for sag, engineers normally shift the die centerpiece downward (see **Fig. 5.** of [41]). Recent work has focused on some of the consequences triggered by this downward decentering [40,41,42,43,1,[2]]. For instance, downward decentering gives rise to a downward force on the mandrel, be the melt elastic or Newtonian (see Eq. (172) of [40]). This paper focuses on heretofore unexplored consequences of downward die decentering, and specifically, on the forces on the die barrel.

Table **I** summarize prior work on flow between eccentric annuli. The reader is alerted to Table **II**, a useful list or errata to the cited articles. Table **III** is a helpful correspondence between the symbols used in this paper, and those of the prior work of Jones [32]. Table **IV** defines the dimensional variables used herein, and Table **V**, the dimensionless ones.

a. Eccentric Cylindrical Coordinates

Eccentric cylindrical coordinates [3], illustrated in Figure 1, consist of two orthogonal sets of cylindrical shells. The first set is defined by the *eccentric radial coordinate*, ξ, and another, by the *eccentric angular coordinate*, θ. The transformations from Cartesian to eccentric cylindrical coordinates are given by:

$$x = a\frac{1-\xi\cos\theta}{1-2\xi\cos\theta+\xi^2}, \quad y = a\frac{\xi\sin\theta}{1-2\xi\cos\theta+\xi^2}, \quad z_C = z \qquad (1),(2),(3)$$

where:

$$a \equiv \delta^{-1}\left(R_o^4 + R_i^4 + \delta^4 - 2R_i^2R_o^2 - 2R_i^2\delta^2 - 2R_o^2\delta^2\right)^{1/2} \qquad (4)$$

where R_i, R_o and δ are the mandrel radius, the extrusion die radius and the eccentricity (see **Fig. 2.** of [40]). Extrudate emerges from the die in the positive z-direction.

Employing Eqs. (A.7-13) of [4] gives us the *scale factors* for coordinates ξ and θ:

$$h_\xi \equiv \frac{a}{1+\xi^2-2\xi\cos\theta}, \quad h_\theta \equiv \frac{a\xi}{1+\xi^2-2\xi\cos\theta} \qquad (5), (6)$$

The differential area relevant to the forces on the barrel is given by:

$$dA_{\theta z} = \frac{a\xi}{1+\xi^2-2\xi\cos\theta}d\theta dz \qquad (7)$$

which we will use in Section II to get the forces on the barrel.

b. The Oldroyd 8-Constant Framework

The Oldroyd 8-constant framework is given by (see Eq. (8.1-2) in [5]; [6,7]):

$$\tau_{ik}+\lambda_1\frac{\mathscr{D}\tau_{ik}}{\mathscr{D}t}+\mu_0\tau_{jj}\dot{\gamma}_{ik}-\mu_1\left(\tau_{ij}\dot{\gamma}_{ik}+\tau_{jk}\dot{\gamma}_{ij}\right)+\nu_1\tau_{jl}\dot{\gamma}_{jl}\delta_{ik}=2\eta_0\left(\dot{\gamma}_{ik}+\lambda_2\frac{\mathscr{D}\dot{\gamma}_{ik}}{\mathscr{D}t}-2\mu_2\dot{\gamma}_{ij}\dot{\gamma}_{jk}+\nu_2\dot{\gamma}_{il}\dot{\gamma}_{jl}\delta_{ik}\right) \quad (8)$$

where δ_{ik} is *Kronecker delta*. This corotational framework has been studied extensively, both in theory [8,9,10,11] and in its applications [12,40,41,42,43]. Eq. (8) reduces exactly to many special cases. We tabulate 18 of these (see Eq. (13)*ff* in [12]). Our work in this paper can thus be applied exactly to any of these 18 popular cases, or for that matter, to any future constitutive equations derived from the corotational framework that is Eq. (8).

The uninitiated may wonder about how well one or the other of the special cases of the Oldroyd 8-constant equation can approximate real polymer melts. Each of the 18 special cases has its own merits, and the details for this comparison can be found in Chapter 7 of [20] and Chapters 7 and 8 of [5]. Furthermore, to estimate the parameters in Eq. (8) from experimental data, see **PROBLEM 7A.1** of [20]. Eq. (8) has also been approximately connected to the Rivlin-Ericksen, Spriggs 6-constant and Giesekus fluids (see Appendix of [13]).

The Oldroyd 8-constant framework has also been closely connected, albeit approximately, with macromolecular theory ([14,15,16]; see Table 1 of [17]; see Eqs. (32) of [18],[19]; see Tables 6.2-1 and 6.2-2 of [20]; Problems 11B.9 and 11B.10 of [21]; §IV and §V. of [22]; §9.5 of [5]).

In Eq. (8), the total stress, rate of strain and vorticity tensors are given by:

$$\pi_{ik}\equiv\tau_{ik}+p\delta_{ik},\ \dot{\boldsymbol{\gamma}}\equiv\tfrac{1}{2}\left[\nabla\mathbf{v}+\left(\nabla\mathbf{v}\right)^{\dagger}\right],\ \boldsymbol{\omega}\equiv\tfrac{1}{2}\left(\nabla\mathbf{v}-\left(\nabla\mathbf{v}\right)^{\dagger}\right) \quad (9),(10),(11)$$

and the corotational derivative for any tensor $\mathbf{b}$, by:

$$\frac{\mathscr{D}\mathbf{b}}{\mathscr{D}t}\equiv\frac{D\mathbf{b}}{Dt}+\boldsymbol{\omega}\cdot\mathbf{b}-\mathbf{b}\cdot\boldsymbol{\omega} \quad (12)$$

In Eq. (9), p is the hydrodynamic pressure, and $\boldsymbol{\delta}$, the *Kronecker delta*.

The Oldroyd 8-constant framework can be remarkably useful in polymer processing when it leads to analytical solutions, as it does for wire coating (Case III in [32]), for a corrugated wire coated through a corrugated die (see Section 3. of [33]; Section 2. of [23]), for plastic pipe extrusion for elliptical pipe ([24,35]), and also for extrusion from an eccentric annular pipe die (Case II in [32],[40],[42,43],[41]). Moreover, the molecularization of the Oldroyd 6-constant fluid is treated in [25].

In steady shear flow, for any special case of Eq. (8), the viscosity function is given by (Eq. (14) of [26])

$$\frac{\eta}{\eta_0}=\frac{1+\left(\sigma_2/\sigma_1\right)\left(\sqrt{\sigma_1}\dot{\gamma}\right)^2}{1+\left(\sqrt{\sigma_1}\dot{\gamma}\right)^2}\equiv\frac{1+\sigma\,\mathrm{Wi}^2}{1+\mathrm{Wi}^2} \quad (13)$$

where

$$\sigma_i\equiv\lambda_i\lambda_i+\mu_0\left(\mu_i-\tfrac{3}{2}\nu_i\right)-\mu_1\left(\mu_i-\nu_i\right),\quad \sigma\equiv\sigma_2/\sigma_1 \quad (14),(15)$$

We will use Eq. (13) [with Eqs. (14) and (15)] in Subsection II.a to calculate the axial force exerted by the fluid on the barrel.

c. Axial Velocity Profile

In plastic pipe extrusion, the flow through the eccentric die is considered to be rectilinear (see Figure 2):

$$\mathbf{v} = \left[0, 0, v_z(\xi, \theta)\right] \tag{16}$$

This problem was solved in eccentric cylindrical coordinates (see "***Worked example: momentum transfer***" of [3]; [40]). We begin by recalling the dimensionless axial velocity profile (Eqs. (48) and (51) in [40]):

$$\breve{v}_z(\xi, \theta) \equiv \frac{4\eta_0}{a^2 P} v_z = v_0 + (1-\sigma) S v_1 \tag{17}$$

where $P \equiv -dp/dz$ is *minus* the axial pressure gradient (the cause for the flow), and:

$$S \equiv \frac{\sigma_1 a^2 P^2}{16\eta_0^2} \tag{18}$$

and where v_0 and v_1 are given in Eq. (19) and (25).

The Newtonian contribution in Eq. (17) is given by:

$$v_0 = \sum_{n=0}^{\infty} \phi_n \cos n\theta - \frac{1}{1 - 2\xi\cos\theta + \xi^2} \tag{19}$$

where:

$$\phi_n = \begin{cases} \alpha_0 + \beta_0 \ln \xi^2 & ;\, n = 0 \\ 2\alpha_n \xi^n + 2\beta_n \xi^{-n} & ;\, n \geq 1 \end{cases} \tag{20}$$

with α_n, β_n, ξ_i and ξ_o given by:

$$\alpha_n = \begin{cases} \dfrac{\xi_i^{\,2} \ln \xi_i^{\,2} + \ln \xi_o^{\,2} - \xi_o^{\,2} \ln \xi_o^{\,2} - \ln \xi_i^{\,2}}{\left(-\ln \xi_o^{\,2} + \xi_o^{\,2} \ln \xi_o^{\,2} + \ln \xi_i^{\,2} - \xi_o^{\,2} \ln \xi_i^{\,2}\right)\left(-1 + \xi_i^{\,2}\right)} & ;\, n = 0 \\ \dfrac{\xi_i^{\,2} \xi_o^{\,2n} - \xi_o^{\,2n} + \xi_i^{\,2n} - \xi_o^{\,2} \xi_i^{\,2n}}{\left(\xi_o^{\,2n} - \xi_o^{\,2n+2} - \xi_i^{\,2n} + \xi_o^{\,2} \xi_i^{\,2n}\right)\left(-1 + \xi_i^{\,2}\right)} & ;\, n \geq 1 \end{cases} \tag{21}$$

$$\beta_n = \begin{cases} \dfrac{\xi_o^{\,2} - \xi_i^{\,2}}{\left(-\ln \xi_o^{\,2} + \xi_o^{\,2} \ln \xi_o^{\,2} + \ln \xi_i^{\,2} - \xi_o^{\,2} \ln \xi_i^{\,2}\right)\left(-1 + \xi_i^{\,2}\right)} & ;\, n = 0 \\ \dfrac{-\xi_i^{\,n} \xi_o^{\,n} \left(\xi_o^{\,2} - \xi_i^{\,2}\right)}{\left(-\xi_o^{\,n} \xi_i^{\,-n} + \xi_o^{\,n+2} \xi_i^{\,-n} + \xi_o^{\,-n} \xi_i^{\,n} - \xi_o^{\,-n+2} \xi_i^{\,n}\right)\left(-1 + \xi_i^{\,2}\right)} & ;\, n \geq 1 \end{cases} \tag{22}$$

where:

$$\xi_i \equiv \frac{\left(R_o^2 - R_i^2 - \delta^2\right) - \left(R_o^4 + R_i^4 + \delta^4 - 2R_i^2 R_o^2 - 2R_i^2\delta^2 - 2R_o^2\delta^2\right)^{1/2}}{2\delta R_i} \tag{23}$$

$$\xi_o \equiv \frac{\left(R_o^2 - R_i^2 + \delta^2\right) - \left(R_o^4 + R_i^4 + \delta^4 - 2R_i^2R_o^2 - 2R_i^2\delta^2 - 2R_o^2\delta^2\right)^{1/2}}{2\delta R_o} \tag{24}$$

Eq. (23) represents the surface of the extrusion die barrel, and Eq. (24), the mandrel (see Figure 2). The non-Newtonian variable in Eq. (17) is given by:

$$v_1 = \sum_{n=0}^{\infty} \psi_n \cos n\theta \tag{25}$$

which can be truncated to:

$$v_1 = \sum_{n=0}^{4} \psi_n \cos n\theta \tag{26}$$

where:

$$\psi_n = \beta_0^3 \psi_n^{(1)} + \beta_0^2 \psi_n^{(2)} + \beta_0 \psi_n^{(3)} + \psi_n^{(4)} \tag{27}$$

with:

$$\psi_n^{(m)} = \begin{cases} \mathrm{A}_0^{(m)} + \mathrm{B}_0^{(m)} \ln \xi^2 + v_{1p,0}^{(m)} & ;\, n = 0 \quad ;\, m = 1,2,3,4 \\ \mathrm{A}_n^{(m)} \xi^n + \mathrm{B}_n^{(m)} \xi^{-n} + v_{1p,n}^{(m)} & ;\, n \geq 1 \quad ;\, m = 1,2,3,4 \end{cases} \tag{28}$$

where:

$$A_n^{(m)} = \begin{cases} \dfrac{\ln \xi_o{}^2 v_{1p,0}^{(m)}\left(\xi_i\right) - \ln \xi_i{}^2 v_{1p,0}^{(m)}\left(\xi_o\right)}{\ln \xi_i{}^2 - \ln \xi_o{}^2}; n = 0 \\ \dfrac{\xi_i{}^{-n} v_{1p,n}^{(m)}\left(\xi_o\right) - \xi_o{}^{-n} v_{1p,n}^{(m)}\left(\xi_i\right)}{\xi_o{}^{-n}\xi_i{}^{n} - \xi_o{}^{n}\xi_i{}^{-n}}; n \geq 1 \end{cases}, \quad B_n^{(m)} = \begin{cases} \dfrac{v_{1p,0}^{(m)}\left(\xi_i\right) - v_{1p,0}^{(m)}\left(\xi_o\right)}{\ln \xi_o{}^2 - \ln \xi_i{}^2}; n = 0 \\ \dfrac{\xi_o{}^{n} v_{1p,n}^{(m)}\left(\xi_i\right) - \xi_i{}^{n} v_{1p,n}^{(m)}\left(\xi_o\right)}{\xi_o{}^{-n}\xi_i{}^{n} - \xi_o{}^{n}\xi_i{}^{-n}}; n \geq 1 \end{cases} \tag{29), (30}$$

and where $v_{1p,n}^{(m)}$ are given in Eqs. (82)–(100) of [40].

II. RESULTS: TARGETED QUANTITIES ON THE BARREL

In this section, we will work out the expression for forces on the barrel. We start with the expression for the magnitude of the rate of strain tensor in eccentric cylindrical coordinates:

$$\dot{\gamma} \equiv \frac{\left(1 - 2\xi\cos\theta + \xi^2\right)}{a\xi} \sqrt{\left(\xi \frac{\partial v_z}{\partial \xi}\right)^2 + \left(\frac{\partial v_z}{\partial \theta}\right)^2} \tag{31}$$

which we nondimensionalize to:

$$\mathrm{Wi} \equiv \sqrt{\sigma_1}\dot{\gamma} = \sqrt{S}\,\frac{1 - 2\xi\cos\theta + \xi^2}{\xi} \sqrt{\left(\xi \frac{\partial \breve{v}_z}{\partial \xi}\right)^2 + \left(\frac{\partial \breve{v}_z}{\partial \theta}\right)^2} \tag{32}$$

We next evaluate Eq. (32) on the die barrel, $\xi = \xi_o$, to (Eq. (121) with Eqs. (122) and (123) of [40]):

$$\mathrm{Wi}_o \equiv \sqrt{\sigma_1}\dot{\gamma}_o = -\sqrt{S}\left[\mathrm{Wi}_0 + \left(1 - \sigma\right) S\, \mathrm{Wi}_1\right] \tag{33}$$

where:

$$\mathrm{Wi}_0=\left(1+\xi_o^2-2\xi_o\cos\theta\right)\left[\sum_{n=0}^{\infty}\phi_n'\big|_{\xi_o}\cos n\theta-\frac{2\cos\theta-2\xi_o}{\left(1-2\xi_o\cos\theta+\xi_o^2\right)^2}\right] \tag{34}$$

$$\mathrm{Wi}_1=\left(1+\xi_o^2-2\xi_o\cos\theta\right)\sum_{n=0}^{4}\psi_n'\big|_{\xi_o}\cos n\theta \tag{35}$$

We will use Eq. (33) [with Eqs. (34) and (35)] to evaluate axial force in Subsection II.a, and for lateral force in Subsection II.b.

For the generalized Newtonian fluid, the expression for the shear stress at the barrel wall is given by:

$$\tau_{\xi z}\left(\xi_o,\theta\right)=\eta\left(\dot{\gamma}_o\right)\dot{\gamma}_o=\eta_0\frac{1+\sigma_2\dot{\gamma}_o^2}{1+\sigma_1\dot{\gamma}_o^2}\dot{\gamma}_o \tag{36}$$

where $\dot{\gamma}_o\equiv\dot{\gamma}\left(\xi_o,\theta\right)$ is the magnitude of the rate of strain tensor at the barrel wall. Nondimensionalizing Eq. (36) gives:

$$\mathbb{S}_o\equiv\frac{\sqrt{\sigma_1}\tau_{\xi z}\left(\xi_o,\theta\right)}{\eta_0}=\frac{1+\sigma\,\mathrm{Wi}_o^2}{1+\mathrm{Wi}_o^2}\mathrm{Wi}_o \tag{37}$$

where Wi_o are given by Eq. (33) [with Eqs. (34) and (35)].

a. Axial Force

The axial force exerted by the fluid on the mandrel per unit length is given by:

$$F_z\equiv\frac{1}{L}\int_A\tau_{\xi z}\left(\xi_o,\theta\right)dA_{\theta z} \tag{38}$$

which can be nondimensionalized to:

$$\mathbb{F}_z\equiv\frac{\sqrt{\sigma_1}F_z}{\eta_0 a}=\frac{1}{L}\int_A\mathbb{S}_o\frac{1}{a}dA_{\theta z} \tag{39}$$

Substituting Eqs. (7) and (37) into Eq. (39) gives:

$$\mathbb{F}_z=\int_0^{2\pi}\frac{1+\sigma\,\mathrm{Wi}_o^2}{1+\mathrm{Wi}_o^2}\frac{\xi_o\,\mathrm{Wi}_o}{1+\xi_o^2-2\xi_o\cos\theta}d\theta \tag{40}$$

which yields no analytical solution. However, for low shear rate at the barrel wall:

$$\dot{\gamma}_o\ll\sqrt{1/\sigma_1} \tag{41}$$

which is often the case in plastic pipe extrusion, substituting Eq. (33) into Eq. (40), and integrating gives:

$$\mathbb{F}_z\equiv\frac{\sqrt{\sigma_1}F_z}{\eta_0 a}=\sqrt{S}\left[\mathbb{F}_{z,0}+\left(1-\sigma\right)S\mathbb{F}_{z,1}\right] \tag{42}$$

where:

$$\mathbb{F}_{z,0}\equiv\frac{-4\pi\left(\xi_o^{\,2}-\xi_i^{\,2}\right)}{\left(-\ln\xi_o^{\,2}+\xi_o^{\,2}\ln\xi_o^{\,2}+\ln\xi_i^{\,2}-\xi_o^{\,2}\ln\xi_i^{\,2}\right)\left(-1+\xi_i^{\,2}\right)}+\frac{4\pi\xi_o^2}{1-2\xi_o^2+\xi_o^4} \tag{43}$$

$$\mathbb{F}_{z,1}\equiv-2\pi\xi_o\sqrt{S}\begin{bmatrix}\beta_0^3\left[2\mathrm{B}_0^{(1)}\xi_o^{-1}+v_{1p,0}'^{(1)}\left(\xi_o\right)\right]+\beta_0^2\left[2\mathrm{B}_0^{(2)}\xi_o^{-1}+v_{1p,0}'^{(2)}\left(\xi_o\right)\right]\\+\beta_0\left[2\mathrm{B}_0^{(3)}\xi_o^{-1}+v_{1p,0}'^{(3)}\left(\xi_o\right)\right]+\left[2\mathrm{B}_0^{(4)}\xi_o^{-1}+v_{1p,0}'^{(4)}\left(\xi_o\right)\right]\end{bmatrix} \tag{44}$$

where β_0 and $\mathrm{B}_0^{(m)}$ are given by Eqs. (22) and (30), and $v_{1p,0}'^{(m)}$ are given by Eqs. (194), (196), (201) and (207) of [40]. Eq. (42) [with Eqs. (43) and (44)] is the main result of this paper. To plot Figure 3, we coded Eqs. (43) and (44) into MATLAB (Version R2012b) on a MacBook Air (1.3 GHz Intel Core i5 processor with 4 GB 1600 MHz DDR3 memory) employing the OS X (Version 10.10.2) operating system. For each point in Figure 3, we find such an evaluation to consume less than a second CPU time.

b. Lateral Force

The lateral force (per unit length) exerted by the fluid on the mandrel is given by:

$$F_x \equiv \frac{1}{L}\int_A \tau_{\xi\xi}\left(\xi_o,\theta\right) dA_{\theta z} \tag{45}$$

which we nondimensionalize to:

$$\mathbb{F}_o \equiv \frac{1}{L}\int_A \mathbb{S}_o d\frac{A_{\theta z}}{a} \tag{46}$$

where:

$$\mathbb{F}_o \equiv \frac{\sqrt{\sigma_1}F_x}{\eta_0 a},\quad \breve{\tau}_{\xi\xi,o} \equiv \frac{\sqrt{\sigma_1}\tau_{\xi\xi}\left(\xi_o,\theta\right)}{\eta_0} \tag{47),(48}$$

The dimensionless shear stress at the barrel is given by (integrating Eq. (23) of [32]):

$$\breve{\tau}_{\xi\xi,o} = \left[\frac{\left(\lambda_1-\mu_1\right)}{\sqrt{\sigma_1}}\frac{1+\sigma\,\mathrm{Wi}_o^2}{1+\mathrm{Wi}_o^2}-\frac{\left(\lambda_2-\mu_2\right)}{\sqrt{\sigma_1}}\right]\mathrm{Wi}_o^2-\frac{1}{2}\frac{\left(\lambda_1-\mu_1-\lambda_2+\mu_2\right)}{\sqrt{\sigma_1}}\left[\sigma\,\mathrm{Wi}_o^2+\left(1-\sigma\right)\ln\left(1+\mathrm{Wi}_o^2\right)\right] \tag{49}$$

Substituting Eqs. (7) and (49) into Eq. (46) gives:

$$\mathbb{F}_o \equiv \int_0^{2\pi}\left[\begin{array}{l}\left[\frac{\left(\lambda_1-\mu_1\right)}{\sqrt{\sigma_1}}\frac{1+\sigma\,\mathrm{Wi}_o^2}{1+\mathrm{Wi}_o^2}-\frac{\left(\lambda_2-\mu_2\right)}{\sqrt{\sigma_1}}\right]\mathrm{Wi}_o^2\\ -\frac{1}{2}\frac{\left(\lambda_1-\mu_1-\lambda_2+\mu_2\right)}{\sqrt{\sigma_1}}\left[\sigma\,\mathrm{Wi}_o^2+\left(1-\sigma\right)\ln\left(1+\mathrm{Wi}_o^2\right)\right]\end{array}\right]\frac{\xi_o}{1+\xi_o^2-2\xi_o\cos\theta}d\theta \tag{50}$$

which yields no analytical solution. However, for low shear rate at the barrel wall, Eq. (41), which is often true in plastic pipe extrusion, substituting Eq. (33) into Eq. (50) gives:

$$\frac{\mathbb{F}_o}{\left[\frac{\left(\lambda_1-\mu_1-\lambda_2+\mu_2\right)}{\sqrt{\sigma_1}}\left(1-\tfrac{1}{2}\sigma\right)\right]} \equiv \int_0^{2\pi}\frac{\xi_o\,\mathrm{Wi}_o^2}{1+\xi_o^2-2\xi_o\cos\theta}d\theta \tag{51}$$

Substituting Eq. (33) into Eq. (51) gives:

$$\frac{\mathbb{F}_o}{\left[\frac{\left(\lambda_1-\mu_1-\lambda_2+\mu_2\right)}{\sqrt{\sigma_1}}\left(1-\tfrac{1}{2}\sigma\right)\right]} \equiv \sqrt{S}\int_0^{2\pi}\frac{\xi_o\left(\mathrm{Wi}_0^2+2\left(1-\sigma\right)S\,\mathrm{Wi}_0\,\mathrm{Wi}_1+\left(1-\sigma\right)^2S^2\,\mathrm{Wi}_1^2\right)}{1+\xi_o^2-2\xi_o\cos\theta}d\theta \tag{52}$$

which can be truncated to:

$$\chi_o \equiv \frac{\mathbb{F}_o}{\left[\frac{\left(\lambda_1-\mu_1-\lambda_2+\mu_2\right)}{\sqrt{\sigma_1}}\left(1-\tfrac{1}{2}\sigma\right)\right]} = \sqrt{S}\left[\chi_0+\left(1-\sigma\right)S\chi_1\right] \tag{53}$$

where:

$$\chi_0 \equiv \xi_o \int_0^{2\pi} \frac{\mathrm{Wi}_0^2}{1+\xi_o^2-2\xi_o\cos\theta}d\theta, \quad \chi_1 \equiv 2\xi_o \int_0^{2\pi} \frac{\mathrm{Wi}_0\,\mathrm{Wi}_1}{1+\xi_o^2-2\xi_o\cos\theta}d\theta \tag{54),(55}$$

where Wi_0 and Wi_1 are given by Eqs. (34) and (35). Eq. (53) [with Eqs. (54) and (55)] is the main result of this paper. Finally, to plot Figure 4 and Figure 5, we code Eq. (53) [with Eqs. (54) and (55)] using the *integral* routine in Matlab 2012b to evaluate the integrals in Eqs. (54) and (55).

III. DISCUSSION

Figure 3 shows the descending dimensionless axial force on the barrel, $\mathbb{F}_z$, as the flow channel narrows. In other words, by holding the inner contour (ξ_i) constant, the axial force increases with outer contour. Whereas the Newtonian contribution to the dimensionless axial force (see Figure 4) increases with the flow channel, the non-Newtonian contribution decreases (see Figure 5**)**. Interestingly, the dimensionless Newtonian contribution barely changes with the flow channel gap, through changing either ξ_i and ξ_o.

IV. WORKED EXAMPLES

Engineers gather the following process details for their high-density polyethylene pipe extrusion line, where the pipe dimensions are $R_o = 0.32\,\mathrm{m}$, $R_i = 0.22\,\mathrm{m}$, $\delta = 0.01\,\mathrm{m}$ with the throughput of $\rho Q = 0.01\,\mathrm{kg/s}$, and the material properties at the operating temperature are $\eta_0 = 1.1\times10^7\,\mathrm{Pa{\cdot}s}$ and $\rho = 900\,\mathrm{kg/m^3}$. From their measured crossover frequency, ω_c, of her $\eta'(\omega)$ and $\eta''(\omega)$ curves at the operating temperature, she estimates a characteristic relaxation time of $\lambda_1 = 1/\omega_c = 1.38\,\mathrm{s}$. They want to calculate the (i) axial, and (ii) lateral force on the barrel

To get the pressure drop per unit length, P, they first calculate $\xi_i = 0.0409$, $\xi_o = 0.0594$, $a = 5.3720\,\mathrm{m}$, $\sigma_1 = 1.9\mathrm{s}^2$, $\sigma_2 = 0$ and $\sigma = 0$ by inserting the given information into, in order, Eqs. (23), (24), (4), (14)–(15). Following the procedure in **§7** of [40] yields the required pressure drop per unit die land length:

$$P = 8.46\times10^5\ \mathrm{Pa/m} \tag{56}$$

and the dimensionless pressure gradient squared:

$$S \equiv \sigma_1 a^2 P^2 / 16\eta_0{}^2 = 0.0203 \tag{57}$$

and thus S^2 is well below one, as it should be (see Eq. (62)*ff* of [40]). Finally, we use Eq. (33) to calculate the deformation rate at top of the barrel wall:

$$\dot{\gamma}_o = \frac{-\sqrt{0.0203}\left[-0.0386+(0.0203)(-0.1204)\right]}{\sqrt{1.9}} \tag{58}$$
$$= 4.24\times10^{-3}$$

which satisfies $\dot{\gamma}_o \ll \sqrt{1/\sigma_1} = 1.38$, as it should.

(i) Interpolating Figure 3 for $\xi_i = 0.0409$ and $\xi_o = 0.0594$ gives $\mathbb{F}_{z,0} = 0.0132$ and $\mathbb{F}_{z,1} = 4.30\times10^{-6}$. Evaluating Eq. (42) yields the axial force on the barrel per unit length:

$$\mathbb{F}_z = \sqrt{0.0203}\left[0.0132+0.0203\left(4.30\times10^{-6}\right)\right] = 0.00190 \tag{59}$$

Using the definition of $\mathbb{F}_z$, Eq. (42), gives:

$$F_z = \frac{\mathbb{F}_z \eta_0 a}{\sqrt{\sigma_1}} = \frac{(0.00190)\left(1.1\times10^7\,\mathrm{N\,m^{-2}\cdot s}\right)(5.372\,\mathrm{m})}{1.38\,\mathrm{s}} = 8.14\times10^4\,\frac{\mathrm{N}}{\mathrm{m}} \tag{60}$$

the dimensional axial force on the barrel per unit length.

(ii) Interpolating Figure 4 and Figure 5 for $\xi_i = 0.0409$ and $\xi_o = 0.0594$ gives $\chi_0 = 0.984$ and $\chi_1 = 3.19\times10^{-7}$. Evaluating Eq. (53) yields the lateral force on the barrel per unit length:

$$\chi_o = 0.0203\left[(0.984)+(1-\sigma)S\left(3.19\times10^{-7}\right)\right] = 0.0200 \tag{61}$$

Using the definition of χ_o, Eq. (53), gives:

$$F_x = \chi_o \eta_0 a \frac{(\lambda_1 - \mu_1 - \lambda_2 + \mu_2)}{\lambda_1^2 + \mu_0\left(\mu_1 - \tfrac{3}{2}\nu_1\right) - \mu_1(\mu_1 - \nu_1)}\left(1 - \tfrac{1}{2}\sigma\right) \tag{62}$$

$$F_x = \frac{\chi_o \eta_0 a}{\lambda_1} = \frac{(0.0200)\left(1.1\times10^7\,\mathrm{N\,m^{-2}\cdot s}\right)(5.372\,\mathrm{m})}{1.38\,\mathrm{s}} = 8.56\times10^5\,\frac{\mathrm{N}}{\mathrm{m}} \tag{63}$$

the upward dimensional lateral force on the barrel per unit length. Finally, from Eq. (58), we see that the deformation rate at the barrel wall also satisfies $\dot{\gamma}_o \ll 1\big/\sqrt{\sigma_1} = 1.38\,\mathrm{s}$, as it should.

V. CONCLUSION

We consider a large diameter plastic pipe extrusion through an eccentric die using the Oldroyd 8-constant fluid. We arrive at analytical expression for our main results for both axial, Eq. (42) [with Eqs. (43) and (44)], and lateral, Eq. (53) [with Eqs. (54) and (55)], forces on the barrel by solving the equation of motion in eccentric cylindrical coordinates using the polymer process partitioning method [42,43]. We find that the lateral force on the barrel is always be upward, be the melt Newtonian or elastic. Our Worked Example shows how to use our main results, Eq. (42) [with Figure 3] and Eq. (53) [with Figure 4 and Figure 5].

VI. ACKNOWLEDGMENT

Giacomin is indebted to the Faculty of Applied Science and Engineering of Queen's University at Kingston, for its support through a Research Initiation Grant (RIG). This research was undertaken, in part, thanks to support from the Canada Research Chairs program of the Government of Canada for the Natural Sciences and Engineering Research Council of Canada (NSERC) Tier 1 Canada Research Chair in Rheology. This research was also undertaken, in part, thanks to support from the NSERC Discovery Grant program of the Government of Canada.

Table I: Literature Review on Flow between Eccentric Annuli.

Authors (year)	Constitutive Model	Coordinates System	Velocity Profile	Extrudate Shape	Shear Stress	Forces: on the extrusion dies	Forces: On the barrel	[Ref.] (Correction to)
Caldwell (1930)	N	bi	$\mathbb{C}$	Σ				[27]
Piercy *et al*. (1933)	N	bi	Σ	Σ				[28]
Oldroyd (1947)	B	ec	Σ					[29]
Heyda (1959)	N	bi	Σ					[30]
Berker (1963)	N	bi						Sect. 23.9 [31]
Jones (1964); Jones and Jones (1966)	O_8	ec	Σ			χ		[32,33]
Snyder *et al*. (1965)	N	bi	Σ		Σ			[34]
Camilleri and Jones (1966)	O_8	ec	Σ					[35]
Guckes (1975)	P	bi		$\aleph$				[36]
Ballal and Rivlin (1975)	RE	bi	Σ					[37]
Zidan and Hassan (1985)	$O^{(2)}$	bi	Σ					[38]
Kolitawong and Giacomin (2001)	P	bi	$\mathbb{C}$	$\mathbb{C}\aleph$	Σ	$\mathbb{F}$		[39]
Saengow *et al.* (2015); Saengow *et al.* (2017); Saengow (2016)	O_8	ec	Σ	$\mathbb{C}\aleph$	$\mathbb{C}\aleph$	$\mathbb{F},\chi$		[40,41]; [42,43]
This paper	O_8	ec					$\mathbb{F},\chi$	[44]

Legend: B ≡ Bingham; O_8 ≡ 8-constant Oldroyd; P ≡ power-law; N ≡ Newtonian; $O^{(2)}$ ≡ Second-order; RE ≡ Rivlin-Ericksen; ec ≡ eccentric cylindrical coordinates; bi ≡ bipolar cylindrical coordinates; $\mathbb{F}$ ≡ axial force; χ ≡ lateral force; Σ ≡ series; $\mathbb{C}$ ≡ closed form; $\aleph$ ≡ numerical; $\mathbb{C}\aleph$ ≡ closed form with integral defined function;

Table II: Errata to Cited Articles.

Ref.	Errata
[8]	In Eqs. (47) and (48), each τ in the integrands should be τ'
[9]	In column 4 of rows 12 and 13, $\lambda_2 = \mu_0 = \mu_1$ should be $\mu_1 = -\lambda_1 ; \lambda_2 = \mu_0$ and $\mu_1 = \lambda_1 ; \lambda_2 = \mu_0$
[11]	After Eq. (20), Ref. [10] should be [13]; Eq. (65) should be $\mathrm{We/De} > \sqrt[h_{\mathbb{N}}]{(h_{\mathbb{N}}+1)!}$; after Eq. (65), $\sqrt[3]{3!}$ should be $\sqrt[4]{5!}$, and $\gamma_0 > 1.82$ should be $\gamma_0 > 3.31$; in Eq. (66), "$20\mathrm{De}^2$" and "$10\mathrm{De}^2 - 50\mathrm{De}^4$" should be "$20\mathrm{De}$" and "$\left(10\mathrm{De} - 50\mathrm{De}^3\right)\mathrm{De}$" and so Fig. 15 through Fig. 17 of [45] replace Figs. 5–7; on the ordinates of Figs. 5-7, $\frac{1}{2}$ should be 2; in Eqs. (76) and (77), $\mathit{\Psi}'$ and $\mathit{\Psi}''$ should be Ψ_1' and Ψ_1''; throughout, $\mathit{\Psi}_1^d$, $\mathit{\Psi}_1'$ and $\mathit{\Psi}_1''$ should be Ψ_1^d, Ψ_1' and Ψ_1''; after Eq. (119), "$(\zeta\alpha)$" should be "$\zeta(\alpha)$"; in Eq. (127), "$\cos\tau$" should be "$(-\cos\tau)$"; after Eq. (136), "Eq. (134)" should be "Eqs. (133) and (135)" and "Eq. (135)" should be "Eqs. (134) and (135)"; after Eq. (143), $\lvert\tau_{yx}\rvert$ should be $\dot{\gamma}$; in Eq. (147), "$n-1$" should be "$n=1$"; in Eqs. (181) and (182), "1,21" should be "1,2"; after Eq. (184) and in Eq. (185), "mp" should be "$1,mp$"; see also [46]
[17]	In Table 1, η_p should be $\eta_0 - \eta_s$; Two and three lines above "**6. STEADY SHEAR FLOW**", "Oldroyd expression for viscosity or normal stresses or extensional viscosity," should be "Oldroyd expressions for $\eta(\dot{\gamma})$, $\Psi_1(\dot{\gamma})$, $\Psi_2(\dot{\gamma})$, $\eta_{\mathrm{E}}(\dot{\varepsilon})$, $\eta'(\omega)$ and $\eta''(\omega)$,".
[21]	Column 3 of rows 3 and 4 of Table IV of [9] correct column 3 of the last two rows in TABLE 7.3-2.
[26]	In Eq. (12), both occurrences of "$\boldsymbol{\tau}$" should be "$\mathbf{b}$"
[32]	In Eqs. (20) and (22a), "*a* const.," should be "a const.,"; In Eq. (15), "$9\sigma_2 \geq \sigma_1 \geq 0$" should be "$9\sigma_2 \geq \sigma_1 \geq 1$"; In Eq. (45), "$w' = w_0 + (1-\sigma)Sw_1 + S^2 w_2 + S^3 w_3 + \ldots$" should be "$w' = w_0 + (1-\sigma)Sw_1 + (1-\sigma)^2 S^2 w_2 + (1-\sigma)^3 S^3 w_3 + \ldots$"; In Eq. (54), "$\psi_n =$" should be "$\Psi_n =$"; In Eq. (3.5), "$\omega_{ij} =$" should be "$\omega_{ik} =$"; In Eq. (16), "$Z^* = x + iy$" should be "$Z^* = x - iy$."; The first term on RHS of Eq. (23) "γ_2" should be "γ^2"; The expression for $F_1^{(4)}$ in Eq. (56), "r^{-4}" should be "$r-4$".
[39]	in Ref. 9 and ***Table 1.***, "Buckes" should be "Guckes"; in Ref. 11 and ***Table 1.***, "1932" should be "1930"; in Ref. 11, "J. J." should be "J., J.".

[45]	From 6th line of **Introduction**, delete "small-amplitude oscillatory shear"; in Eq. (6), "38725" should be "38728"; in Ref. [22], "[23]" should be "[21]". In Eq. (27), " $P_6^4 c_4$ " should be " $\frac{7}{396} P_6^4 c_4$ "; In Eq. (32), " $\frac{1}{63504}$ " should be " $\frac{-1}{63504}$ "; In Eq. (33), " $\frac{-1}{6\lambda}\frac{1}{432}\frac{3}{49}\frac{20}{7}$ " should be " $\frac{+1}{6\lambda}\frac{1}{432}\frac{3}{49}\frac{20}{7}$ "; In Eq. (35), " $\frac{-1}{74088}$ " should be " $\frac{+1}{74088}$ "

Table III: Symbol Correspondence between This Paper and Jones [32].

Variable name	This paper	Jones [32]
Axial velocity	v_z	w
Axial velocity, dimensionless	$\breve{v}_z$	w'
Axial velocity, Newtonian contribution	v_0	w_0
Axial velocity, non-Newtonian variable	v_1	w_1
Confocal length	a	d
Contour, inner	ξ_i	a
Contour, outer	ξ_o	b
Eccentric angular cylindrical coordinate	θ	φ
Eccentric radial cylindrical coordinate	ξ	r
Eccentricity	δ	h
Extra stress tensor	τ_{ij}	p'_{ij}
Magnitude of rate of strain tensor	$\dot{\gamma}$	γ
Steady shear viscosity function	$\eta(\dot{\gamma})$	$F(\gamma)$

Table IV: Dimensional Variables

Name	Unit	Symbol
Cartesian Coordinates [Eqs. (1)–(3)]	L	x, y, z_C
Eccentric Cylindrical Coordinate, Axial [Figure 1]	L	z
Confocal Length [Eq. (4)]	L	a
Radius, mandrel [Eq. (4)]	L	R_i
Radius, extrusion die [Eq. (4)]	L	R_o
Eccentricity [Eq. (4)]	L	δ
Differential area $d\theta dz$ [Eq. (7)]	L^2	$dA_{\theta z}$
Extra stress, ijth component* [Eq. (9)]	M/Lt^2	τ_{ik}
Oldroyd constant, relaxation time [Eq. (8)]	t	λ_1
Oldroyd constant, retardation time [Eq. (8)]	t	λ_2
Oldroyd constants [Eq. (8)]	t	$\mu_0, \mu_1, \mu_2, \nu_1, \nu_2$
Vorticity tensor [Eq. (11)]	t^{-1}	$\boldsymbol{\omega}$
Viscosity, zero shear [Eq. (13)]	M/Lt	$\eta_0 = \lim_{\dot{\gamma} \to 0} \eta(\dot{\gamma})$
Rate of strain tensor [Eq. (10)]	t^{-1}	$\dot{\boldsymbol{\gamma}}$
Rate of strain, ijth component [Eq. (8)]	t^{-1}	$\dot{\gamma}_{ij}$
Hydrodynamics pressure [(9)]	M/Lt^2	p
Total stress tensor, ijth component [Eq. (9)]	M/Lt^2	π_{ij}
Oldroyd steady shear constants [Eq. (14)	t^2	σ_1, σ_2
Velocity vector, ith component [Eq. (16)]	L/t	$\mathbf{v}, v_i$
Minus of the axial pressure gradient [Eq. (17)]	M/L^2t^2	P
Rate of strain tensor, magnitude [Eq. (31)]	t^{-1}	$\dot{\gamma}$
Rate of strain tensor, magnitude, outer contour [Eq. (33)]	t^{-1}	$\dot{\gamma}_o$
Force on the barrel per unit length, axial [Eq. (38)]	M/t^2	F_z
Force on the barrel per unit length, lateral [Eq. (45)]	M/t^2	F_x

Legend: $M \equiv$ mass; $L \equiv$ length; $t \equiv$ time; $T \equiv$ temperature

*Where τ_{ij} is the force exerted in the jth direction on a unit area of fluid surface of constant x_i by fluid in the region lesser x_i on fluid in the region greater x_i (see ''Note on the Sign Convention for the Stress Tensor''on pp. 19–20 of [4], or pp. 24–25 of [47]).

Table V: Dimensionless Variables and Groups

Name	Symbol
Eccentric coordinate, radial [Figure 1]	ξ
Eccentric coordinate, radial, inner contour [Figure 2]	ξ_i
Eccentric coordinate, radial, outer contour [Figure 2]	ξ_o
Eccentric coordinate, angular [Figure 1]	θ
Scale factor, radial [Eq. (5)]	h_ξ
Scale factor, angular [Eq. (6)]	h_θ
Oldroyd constant ratio [Eq. (15)]	σ
Axial velocity [Eq. (17)]	$\breve{v}_z$
Squared pressure gradient [Eq. (18)]	S
Axial velocity, Newtonian contribution [Eq. (19)]	v_0
Axial velocity, non-Newtonian contribution [Eq. (25)]	v_1
Spatial function of axial velocity, Newtonian contribution, nth harmonic [Eq. (20)	ϕ_n
Spatial function of axial velocity, non-Newtonian variable, nth harmonic [Eq. (27)]	ψ_n
Spatial function of axial velocity, non-Newtonian variable, nth harmonic, mth group [Eq. (27)]	$\psi_n^{(m)}$
Axial velocity, non-Newtonian variable, particular solution, nth harmonic, mth group	$v_{1p,n}^{(m)}$
Integration coefficient, Newtonian contribution, n-th harmonic [Eqs. (21), (22), (29) and (30)]	$\alpha_n, \beta_n, A_n, B_n$
Weissenberg number [Eq. (32)]	Wi
Weissenberg number, outer contour [Eq. (33)]	Wi_o
Weissenberg number, outer contour, Newtonian contribution [Eq. (34)]	Wi_0
Weissenberg number, outer contour, non-Newtonian contribution [Eq. (33)]	Wi_1
Shear stress, outer contour [Eq. (37)]	$\mathbb{S}_o$
Axial force, outer contour [Eq. (42)]	$\mathbb{F}_z$
Axial force, outer contour, Newtonian contribution [Eq. (43)]	$\mathbb{F}_{z,0}$
Axial force, outer contour, non-Newtonian contribution [Eq. (44)]	$\mathbb{F}_{z,1}$
Normal stress, outer contour [Eq. (48)]	$\breve{\tau}_{\xi\xi,o}$
Lateral force, outer contour [Eq. (47)]	$\mathbb{F}_o$
Lateral force on the barrel [Eq. (53)]	χ_o
Lateral force on the barrel, Newtonian contribution [Eq. (54)]	χ_0
Lateral force on the barrel, non-Newtonian contribution [Eq. (55)]	χ_1

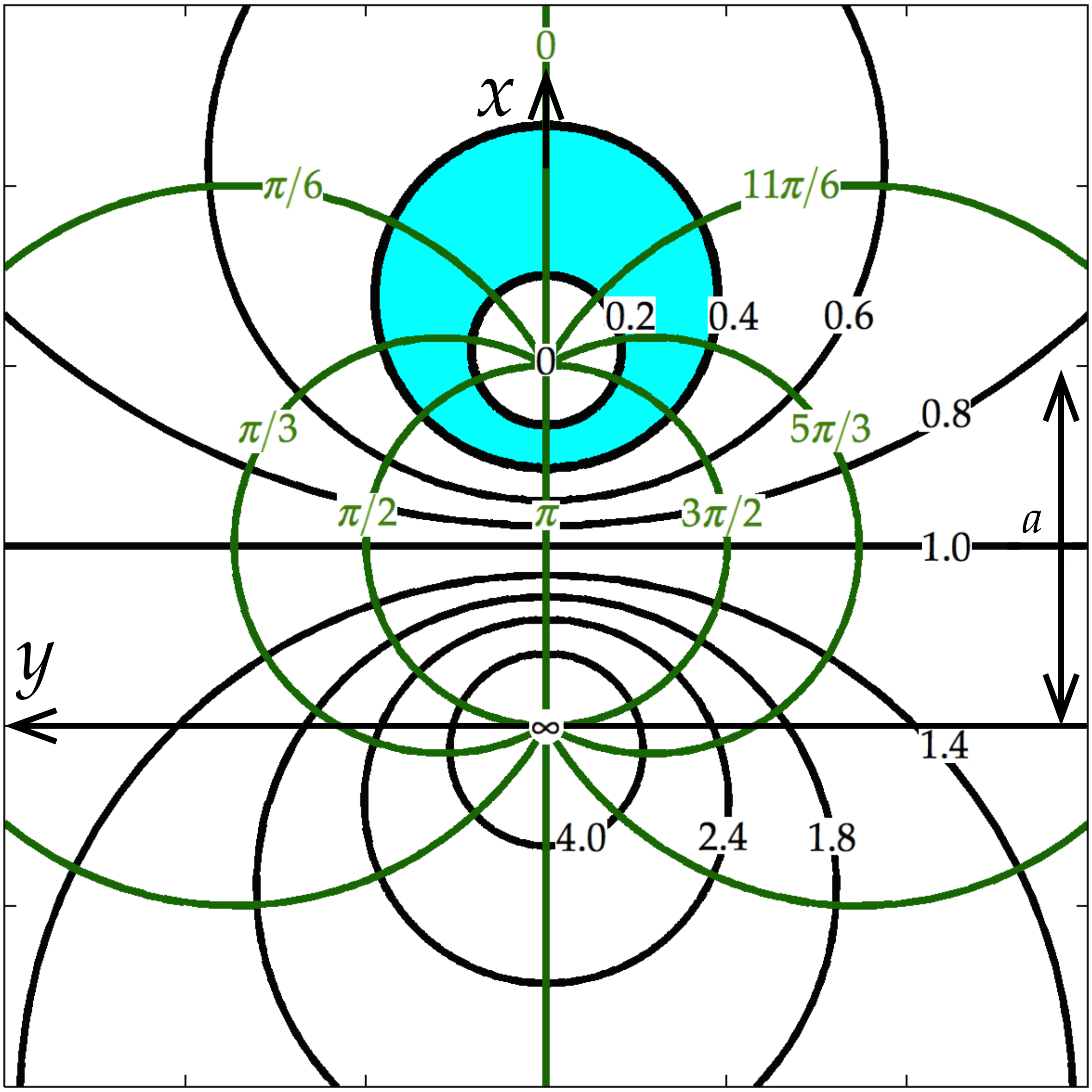

Figure 1: Eccentric cylindrical coordinates showing the circles of constant eccentric radial coordinate (**black**), ξ, and the circles of constant eccentric angular coordinate (**green**), θ [Eqs. (1) and (2)]. Cyan eccentric pipe, between $\xi_i = 0.2$ and $\xi_o = 0.4$, illustrates an example of a pipe extrudate.

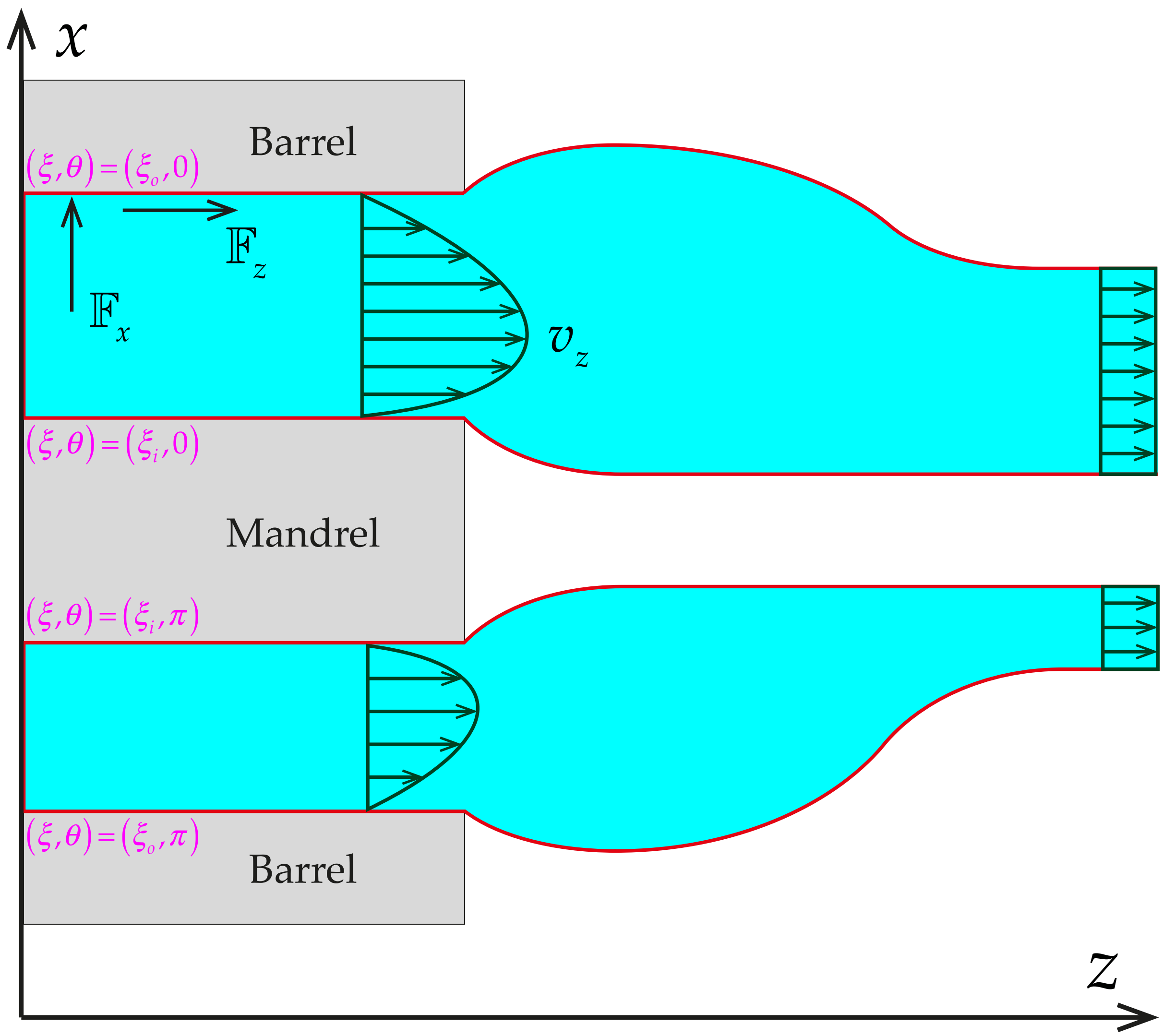

Figure 2: Flow of polymer melt through eccentric extrusion die. The mandrel is shifted downward, by the value of δ, for sag compensation. ξ_i and ξ_o are mandrel and barrel contours. $\theta = 0$ and $\theta = \pi$ are the eccentric angular cylindrical position at the top and to bottom.

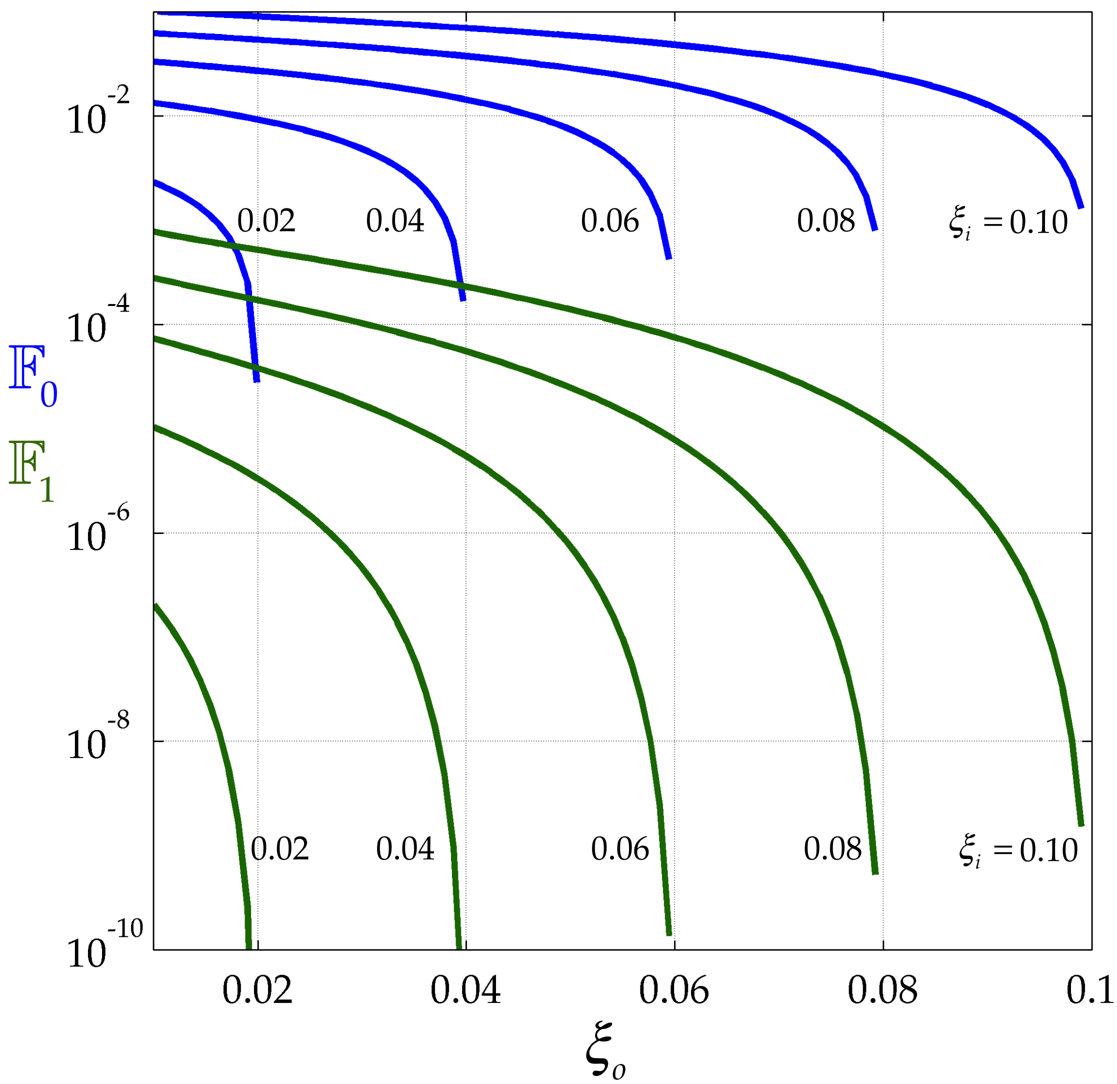

Figure 3: Axial force exerted by the fluid on the barrel [Eqs. (43), (44)].

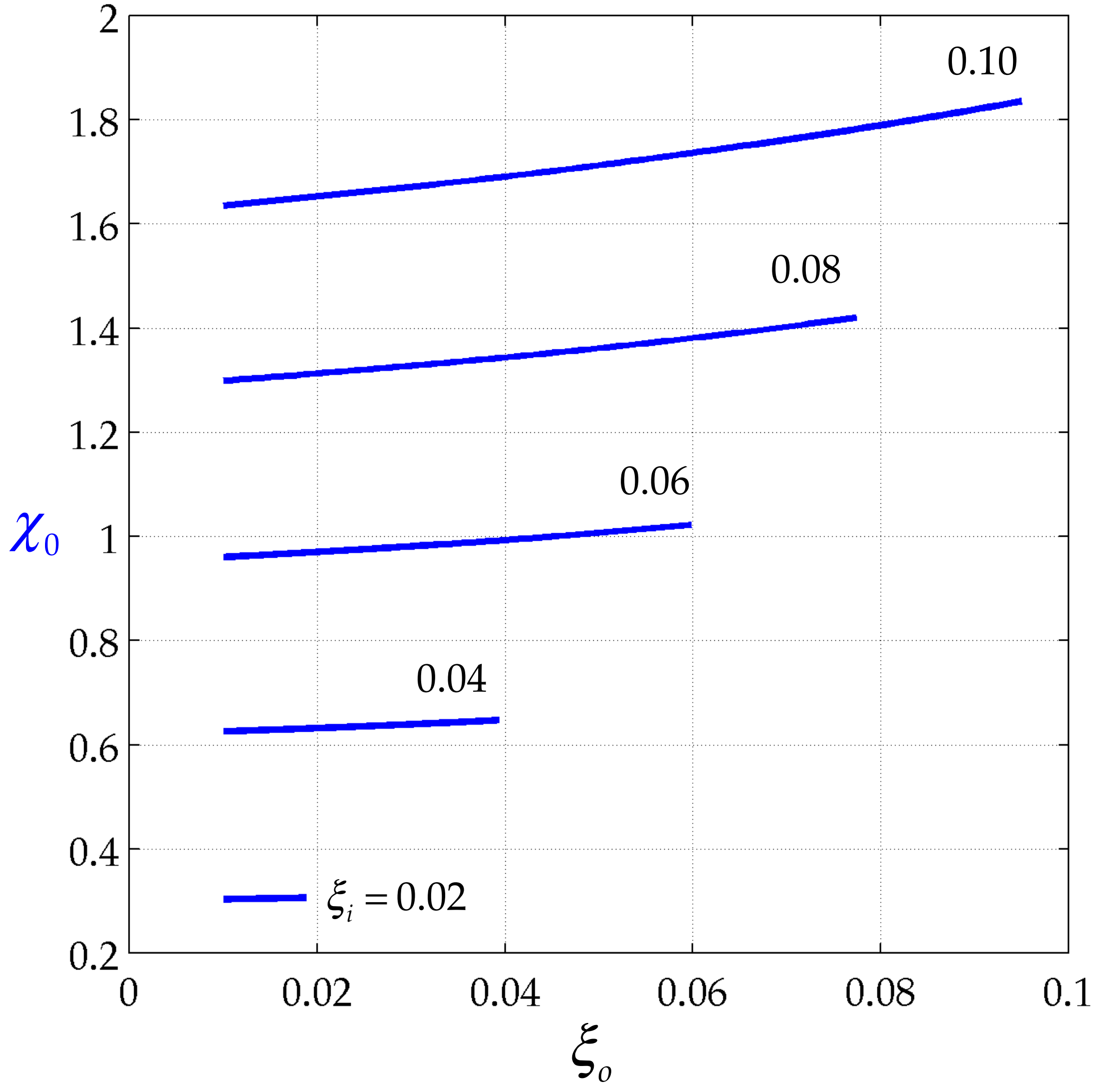

Figure 4: Newtonian contribution, χ_0, to the lateral force on the barrel [Eq. (54)].

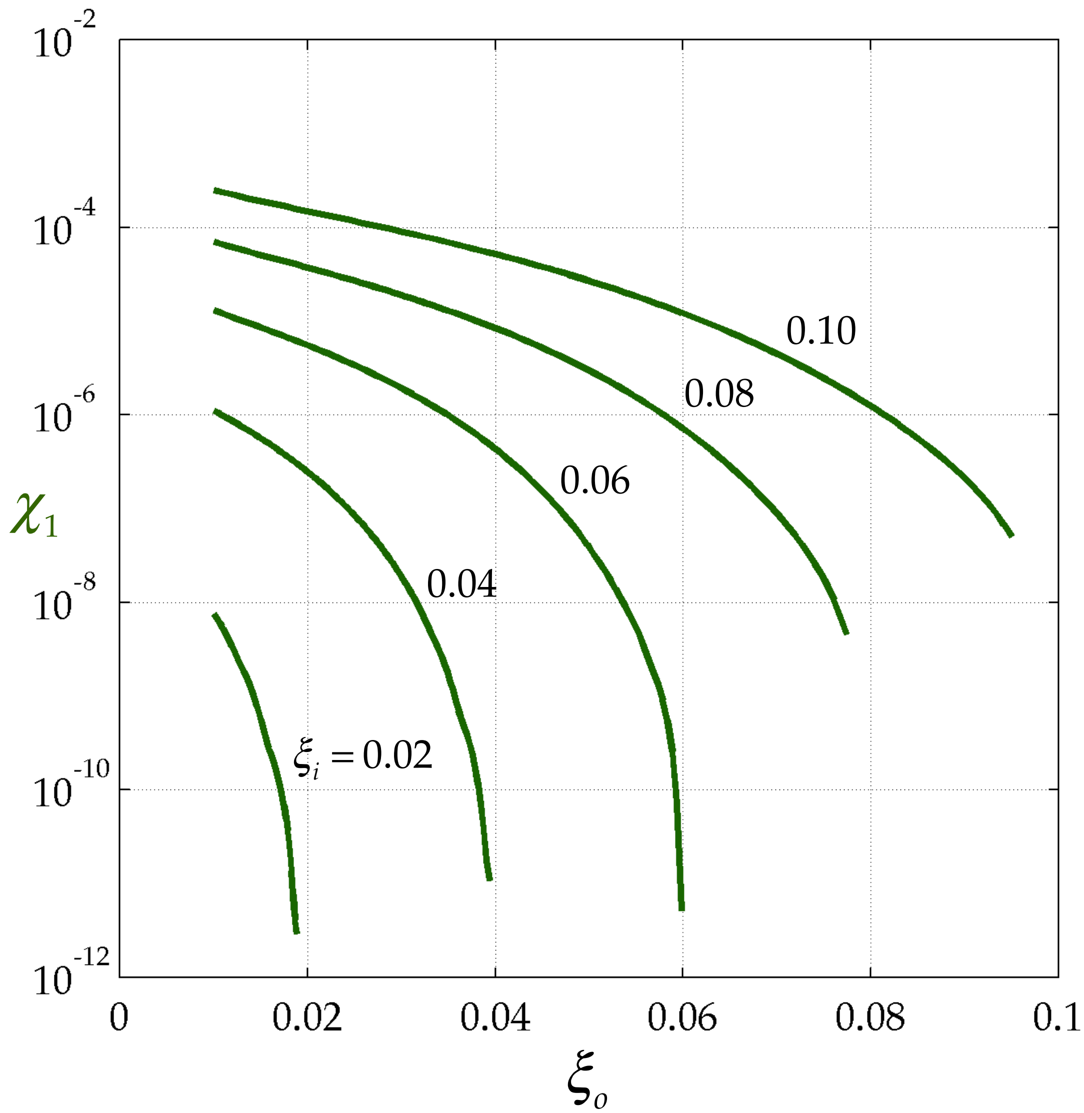

Figure 5: Non-Newtonian contribution, χ_1, to the lateral force on the barrel [Eq. (55)].

VII. REFERENCES

[1] Githuku, D.N. and A.J. Giacomin, "Simulation of Slump in Plastic Pipe Extrusion," *Journal of Engineering Materials and Technology*, **114**(1), 81–83 (1992).

[2] Githuku, D.N., *Simulation of Sag During the Solidification of Extruded Plastic Pipe*, PhD Thesis, Texas A&M University, Mechanical Engineering Dept., College Station, TX (February, 1992)

[3] Gilbert, P.H., C. Saengow and A.J. Giacomin, "Transport Phenomena in Eccentric Cylindrical Coordinates," *AIChE Journal*, doi: 10.1002/aic.15671 (March, 2017).

[4] Bird, R.B., W.E. Stewart and E.N. Lightfoot, *Transport Phenomena*, Revised 2nd ed., Wiley & Sons, New York (2007).

[5] Bird, R. B., R.C. Armstrong and O. Hassager, *Dynamics of Polymeric Liquids*, Vol. 1, 1st ed., Wiley, New York (1977).

[6] Oldroyd, J. G., "Non-Newtonian Effects in Steady Motion of Some Idealized Elastico-Viscous Liquids," In *Proceedings of the Royal Society of London A: Mathematical, Physical and Engineering Sciences*, **245**(1241), 278–297 (1958).

[7] Imran, A., A.M. Siddiqui and M.A. Rana, "Flow of Oldroyd 8-constant fluid in a scraped surface heat exchanger," *The European Physical Journal Plus*, **131**(12), 446 (2016).

[8] Saengow, C., A.J. Giacomin and C. Kolitawong, "Exact Analytical Solution for Large-Amplitude Oscillatory Shear Flow," *Macromolecular Theory and Simulations*, **24**(4), 352–392 (2015).

[9] Saengow, C., A.J. Giacomin and C. Kolitawong, "Exact Analytical Solution for Large-Amplitude Oscillatory Shear Flow from Oldroyd 8-Constant Framework: Shear Stress," *Physics of Fluids*, **29**(4), 043101 (2017).

[10] Saengow, C. and A.J. Giacomin, "Normal Stress Differences from Oldroyd 8-Constant Framework: Exact Analytical Solution For Large-Amplitude Oscillatory Shear Flow," *Physics of Fluids*, accepted (2017).

[11] Giacomin, A.J., R.B. Bird, L.M. Johnson and A.W. Mix, "Large-Amplitude Oscillatory Shear Flow from the Corotational Maxwell Model," *Journal of Non-Newtonian Fluid Mechanics*, **166**(19–20), 1081–1099 (2011).

[12] Saengow, C. and A.J. Giacomin, "Exact Solutions for Oscillatory Shear Sweep Behaviors of Complex Fluids from the Oldroyd 8-Constant Framework," *Physics of Fluids*, accepted (June 6, 2017).

[13] Caswell, B., "The Effect of Finite Boundaries on the Motion of Particles in Non-Newtonian Fluids," *Chemical Engineering Science*, **25**(7), 1167–1176 (1970).

[14] Abdel-Khalik, S.I., O. Hassager and R.B. Bird, "The Goddard Expansion and the Kinetic Theory for Solutions of Rodlike Macromolecules," *The Journal of Chemical Physics*, **61**(10), 4312–4316 (1974).

[15] Bird, R.B., O. Hassager and S.I. Abdel-Khalik, "Co-Rotational Rheological Models and the Goddard Expansion," *AIChE Journal*, **20**(6), 1041–1066 (1974).

[16] Bird, R.B., "A Modification of the Oldroyd Model for Rigid Dumbbell Suspensions with Brownian Motion," *Zeitschrift für angewandte Mathematik und Physik (ZAMP)*, **23**(1), 157–159 (1972).

[17] Bird, R.B. and A.J. Giacomin, "Polymer Fluid Dynamics: Continuum and Molecular Approaches," *Annual Review of Chemical and Biomolecular Engineering*, **7**, 479–507 (2016).

[18] Lumley, J.L., "Applicability of the Oldroyd Constitutive Equation to Flow of Dilute Polymer Solutions," *Physics of Fluids*, **14**(11), 2282–2284 (1971).

[19] Lumley, J.L., "Erratum: Applicability of the Oldroyd Constitutive Equation to Flow of Dilute Polymer Solutions," *Physics of Fluids*, **15**(11), 2081–2081 (1972).

[20] Bird, R. B., R.C. Armstrong and O. Hassager, *Dynamics of Polymeric Liquids*, Vol. 1, 2nd ed., Wiley, New York (1987).

[21] Bird, R.B., O. Hassager, R.C. Armstrong and C.F. Curtiss, *Dynamics of Polymeric Liquids*, Vol. 2, 1st ed., Wiley, New York (1977).

[22] Bird, R.B. and R.C. Armstrong, "Time-Dependent Flows of Dilute Solutions of Rodlike Macromolecules," *The Journal of Chemical Physics*, **56**(7), 3680–3682 (1972).

[23] Jones, R.S., "Flow of an Elastico-Viscous Liquid in a Corrugated Pipe," *Journal de Mécanique*, **6**(3), 443–448 (1967).

[24] Jones, J.R., "Flow of Elastico-Viscous Liquids in Pipes with Cores (PART TWO)," *Journal de Mécanique*, **4**(1), 121–132 (1965).

[25] Giacomin, A.J. and C. Saengow, "Molecular Continua for Polymeric Liquids in Large-Amplitude Oscillatory Shear Flow," PRG Report No. 030, QU-CHEE-PRG-TR--2017-30, Polymers Research Group, Chemical Engineering Dept., Queen's University, Kingston, CANADA (May, 2017), pp. 1–4.

[26] Saengow, C., A.J. Giacomin, P.H. Gilbert and C. Kolitawong, "Reflections on Inflections," *Korea-Australia Rheology Journal*, **27**(4), 267–285 (2015).

[27] Caldwell, J.J., "The Hydraulic Mean Depth as a Basis for Form Comparison in the Flow of Fluids in Pipes," *Journal of The Royal Technical College (Glasgow)*, **2**, 203–220 (1930).

[28] Piercy, N.A.V., M.S. Hooper and H.F. Winny, "LIII. Viscous Flow Through Pipes with Cores," *The London, Edinburgh, and Dublin Philosophical Magazine and Journal of Science* **15**(99), 647–676 (1933).

[29] Oldroyd, J.G., "Rectilinear Plastic Flow of a Bingham Solid I. Flow Between Eccentric Circular Cylinders in Relative Motion," *Mathematical Proceedings of the Cambridge Philosophical Society*, **43**(4), 521–532 (1947).

[30] Heyda, J.F. "A Green's Function Solution for the Case of Laminar Incompressible Flow Between Non-Concentric Circular Cylinders, " *Journal of the Franklin Institute*, **267**(1), 25–34 (1959).

[31] Berker, R. "*Intégration des Équation du Movement d'un Fluide Visqueux Incompressible*," *Handbuch Der Phyisik*, Stromungsmechanik II, Flugge, S., Ed. Springer-Verlag, Berlin, **VIII**/2, (1963).

[32] Jones, J.R., "Flow of Elastic-Viscous Liquids in Pipes with Cores (PART ONE)," *Journal de Mécanique*, **3**(1), 79–99 (March, 1964).

[33] Jones, J.R. and R.S. Jones, "Flow of Elastico-Viscous Liquids in Pipes with Cores (Part III)," *Journal de Mécanique*, **5**(3), 375–395 (1966).

[34] Snyder, William T., and G.A. Goldstein, "An Analysis of Fully Developed Laminar Flow in an Eccentric Annulus," *AIChE Journal*, **11**(3), 462–467 (1965).

[35] Camilleri, C.J. and J.R. Jones, "The Effect of a Pressure Gradient on the Secondary Flow of Non-Newtonian Liquids between Non-Intersecting Cylinders," *Zeitschrift für angewandte Mathematik und Physik*, **17**(1), 78–90 (1966).

[36] Guckes, T.L, "Laminar Flow of Non-Newtonian Fluids in an Eccentric Annulus," *Journal of Manufacturing Science and Engineering*, **97**(2), 498–506 (1975).

[37] Ballal, B.Y., and R.S. Rivlin, "Flow of a Newtonian Fluid between Eccentric Rotating Cylinders: Inertial Effects," *Archive for Rational Mechanics and Analysis*, **62**(3), 237–294 (1976).

[38] Zidan, M. and A.A. Hassan, "Flow of a Viscoelastic Fluid between Eccentric Cylinders," *Rheologica acta*, **24**(2), 127–133 (1985).

[39] Kolitawong, C. and A.J. Giacomin, "Axial Flow Between Eccentric Cylinders," *Polymer-Plastics Technology and Engineering*, **40**(3), 373–394 (2001).

[40] Saengow, C., A.J. Giacomin and C. Kolitawong, "Extruding Plastic Pipe from Eccentric Dies," *Journal of Non-Newtonian Fluid Mechanics*, **223**, 176–199 (2015).

[41] Saengow, C., A.J. Giacomin and C. Kolitawong, "Knuckle Formation from Melt Elasticity in Plastic Pipe Extrusion," *Journal of Non-Newtonian Fluid Mechanics*, **242**, 11–22 (2017).

[42] Saengow, C., *Polymer Process Partitioning: Extruding Plastic Pipe*, PhD Thesis, Chemical Engineering Department, Queen's University, Kingston, CANADA (2016)

[43] Saengow, C., *Polymer Process Partitioning Approach: Plastic Pipe Extrusion*, PhD Thesis, Mechanical and Aerospace Engineering Department, King Mongkut's University of Technology North Bangkok, THAILAND (2016).

[44] Saengow, C. and A.J. Giacomin, "Loads on Die Barrel and Fluid Elasticity in Plastic Pipe Extrusion," PRG Report No. 033, QU-CHEE-PRG-TR--2017-33, Polymers Research Group, Chemical Engineering Dept., Queen's University, Kingston, CANADA (July, 2017), pp. 1–27.

[45] Schmalzer, A.M. and A.J. Giacomin, "Orientation in Large-Amplitude Oscillatory Shear," Cover Article, *Macromolecular Theory and Simulations*, **24**(3), 171, 181–207 (2015).

[46] Giacomin, A.J., R.B. Bird, L.M. Johnson and A.W. Mix,'Corrigenda: "Large-Amplitude Oscillatory Shear Flow from the Corotational Maxwell Model," [Journal of Non-Newtonian Fluid Mechanics, **166**, 1081–1099 (2011)],' *Journal of Non-Newtonian Fluid Mechanics*, **187–188**, 48–48 (2012).

[47] Bird, R.B., W.E. Stewart, E.N. Lightfoot and D.J. Klingenberg, *Introductory Transport Phenomena*, John Wiley & Sons, New York (2015).